Inorg. Chem. **2004**, *43*, 2234−2236

Inorganic Chemistry
Communication

mer-[Fe^{III}(bpca)(CN)$_3$]$^-$: A New Low-Spin Iron(III) Complex to Build Heterometallic Ladder-like Chains

Rodrigue Lescouëzec,[1a] Jacqueline Vaissermann,[1b] Luminita Marilena Toma,[1a] Rosa Carrasco,[1a] Francesc Lloret,[1a] and Miguel Julve*,[1a]

Departament de Química Inorgànica/Instituto de Ciencia Molecular, Facultat de Química de la Universitat de València, Dr. Moliner 50, 46100-Burjassot, València, Spain, and Laboratoire de Chimie Inorganique et Matériaux Moléculaires, Unité CNRS 7071, Université Pierre et Marie Curie, 4 Place Jussieu, Case 42, 75252 Paris Cedex 05, France

Received September 25, 2003

The novel mononuclear complex PPh$_4$-*mer*-[Fe^{III}(bpca)$_3$(CN)$_3$]·H$_2$O (**1**) [PPh$_4^+$ = tetraphenylphosphonium cation and bpca = bis(2-pyridylcarbonyl)amidate anion] and ladder-like chain compound {[Fe^{III}(bpca)(μ-CN)$_3$Mn^{II}(H$_2$O)$_3$] [Fe^{III}(bpca)(CN)$_3$]}·3H$_2$O (**2**) have been prepared and characterized by X-ray diffraction analysis. Compound **1** is a low-spin iron(III) compound with three cyanide ligands in *mer* arrangement and a tridentate N-donor ligand building a distorted octahedral environment around the iron atom. Compound **2** is an ionic salt made up of cationic ladder-like chains {[Fe^{III}(bpca)(μ-CN)$_3$Mn^{II}(H$_2$O)$_3$]}$^+$ and uncoordinated anions [Fe^{III}(bpca)$_3$(CN)$_3$]$^-$. The magnetic properties of **2** correspond to those of a ferrimagnetic chain with significant intrachain antiferromagnetic coupling between the low-spin iron(III) centers and the high-spin manganese(II) cations. This compound exhibits ferrimagnetic ordering below 2.0 K.

Efforts to extend the vast chemistry of the polyfunctional Prussian-blue-type compounds[2−5] into the molecular regime, mainly to get a deeper knowledge and a better control of their magnetic properties, have prompted several research groups to design new cyanide-bearing mononuclear six-coordinate metal complexes of formula [M(L)$_y$(CN)$_x$]$^{(x-m)-}$ (M is a first row transition metal ion and L is a polydentate capping ligand) that can act as ligands toward fully solvated or partially blocked metal ions. Some selected recent examples that illustrate the diversity of novel low-dimensional structures with interesting and/or novel magnetic properties are the following: (i) high-nuclearity metal−cyanide cages where L is a neutral tridentate nitrogen donor which is coordinated to the metal ion in *fac* position;[6] (ii) high-spin homo- and heterometallic tetranuclear complexes with intramolecular ferromagnetic coupling;[7,8] (iii) bimetallic chains [{Fe^{III}(L)(CN)$_4$}$_2$M^{II}(H$_2$O)$_2$]·4H$_2$O [M = Mn, Co, and Zn with L = 1,10-phenantholine (phen); M = Co with L = 2,2′-bipyridine (bipy)] where intrachain antiferro- (M = Mn)[9] and ferromagnetic (M = Co)[10] interactions occur, the cobalt derivatives showing slow magnetic relaxation and hysteresis effects which are characteristic of "single chain magnets";[11] (iv) double chains [{Fe^{III}(bipy)(CN)$_4$}$_2$M^{II}(H$_2$O)]·MeCN·$^1/_2$H$_2$O (M = Mn and Co)[12] resulting from the condensation of two of the previous chains where the cobalt compound presents intrachain ferro- and interchain antiferromagnetic interactions and a field-induced transition ($H_c \geq 600$ G and $T_c \leq 7$ K) from an antiferromagnetic to a ferromagnetic ground state; (v) finally, the two-dimensional cyanide bridged compound {[Mn(H$_2$O)$_2$[Mn(bpym)(H$_2$O)]$_2$ [Fe(CN)$_6$]$_2$}$_n$ (bpym = 2,2′-bipyrimidine) which exhibits canted ferrimagnetism wit $T_c = 11$ K.[13]

In our efforts to design new cyanide-bearing paramagnetic precursors to be used as ligands, we have prepared the mono-

---

* To whom correspondence should be addressed. E-mail: miguel.julve@uv.es.

(1) (a) Universitat de València. (b) Université Pierre et Marie Curie.

(2) Dunbar, K. M.; Heintz, R. A. *Prog. Inorg. Chem.* **1997**, *45*, 283 and references therein.

(3) (a) Verdaguer, M.; Bleuzen, A.; Marvaud, V.; Vaissermann, J.; Seuleiman, M.; Desplanches, C.; Scuiller, A.; Train, C.; Garde, R.; Gelly, G.; Lomenech, C.; Rosenman, I.; Veillet, R.; Cartier, C.; Villain, F. *Coord.. Chem. Rev.* **1999**, *190−192*, 1023. (b) Escax, V.; Bleuzen, A.; Cartier dit Moulin, C.; Villain, F.; Goujon, A.; Varret, F.; Verdaguer, M. *J. Am. Chem. Soc.* **2001**, *123*, 12536. (c) Champion, G.; Escax, V.; Cartier dit Moulin, C.; Bleuzen, A.; Villain, F.; Baudelet, F.; Dartyge, E.; Verdaguer, M. *J. Am. Chem Soc.* **2001**, *123*, 12544. (d) Garde, R.; Villain, F.; Verdaguer, M. *J. Am. Chem. Soc.* **2002**, *124*, 10531.

(4) Sato, O.; Hayami, S.; Einaga, Y.; Gu, Z.-Z. *Bull. Chem. Soc. Jpn.* **2003**, *76*, 443.

(5) Widman, A.; Kahlert, H.; Petrovic-Prelevic, I.; Wulff, H.; Yakhmi, J. V.; Bagkar, N.; Scholz, F. *Inorg. Chem.* **2002**, *41*, 5706.

(6) Yang, J. Y.; Shores, M. P.; Sokol, J. J.; Long, J. R. *Inorg. Chem.* **2003**, *42*, 1403 and references therein.

(7) Lescouezëc, R.; Vaissermann, J.; Lloret, F.; Julve, M.; Verdaguer, M. *Inorg. Chem.* **2002**, *41*, 5943.

(8) (a) Oshio, H.; Tamada, O.; Onodera, H.; Ito, T.; Ikoma, T.; Tero-Kubota, S. *Inorg. Chem.* **1999**, *38*, 5686. (b) Oshio, H.; Yamamoto, M.; Ito, T. *Inorg. Chem.* **2002**, *41*, 5817.

(9) Lescouëzec, R.; Lloret, F.; Julve, M.; Vaissermann, J.; Verdaguer, M.; Llusar, R.; Uriel, S. *Inorg. Chem.* **2001**, *40*, 2065.

(10) Lescouëzec, R.; Vaissermann, J.; Ruiz-Pérez, C.; Lloret, F.; Carrasco, R.; Julve, M.; Verdaguer, M.; Dromzee, Y.; Gatteschi, D.; Wernsdorfer, W. *Angew. Chem., Int. Ed.* **2003**, *42*, 1483.

(11) (a) Caneschi, A.; Gatteschi, D.; Lalioti, N.; Sangregorio, C.; Sessoli, R.; Venturi, G.; Vindigni, A.; Rettori, A.; Pini, M. G.; Novak, M. A. *Angew. Chem., Int. Ed.* **2001**, *40*, 1760. (b) Clérac, R.; Miyasaka, H.; Yamashita, M.; Coulon, C. *J. Am. Chem. Soc.* **2002**, *124*, 12387.

(12) Toma, L. M.; Lescouëzec, R.; Lloret, F.; Julve, M.; Vaissermann, J.; Verdaguer, M. *Chem. Commun.* **2003**, 1850.

10.1021/ic030284z CCC: $27.50

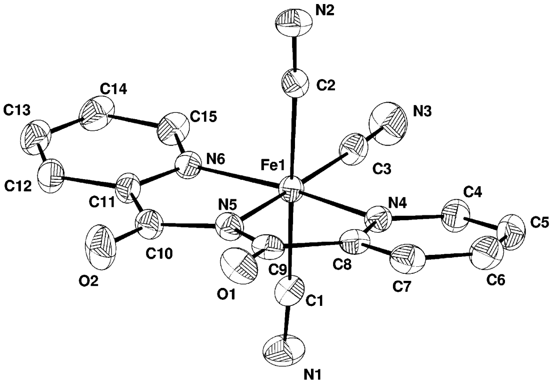

Figure 1. A view of the anion of **1** showing the atom numbering (thermal ellipsoids are at the 30% probability level). Selected bond lengths [Å] and angles [deg]: Fe(1)−C 1.937(3)−1.951(3), Fe(1)−N 1.893(2)−1.959(2), C(1)−Fe(1)−C(2) 174.7(1), C(3)−Fe(1)−N(5) 179.1(1), N(4)−Fe(1)−N(5) 82.7(1), N(4)−Fe(1)−N(6) 165.7(1), N(5)−Fe(1)−N(6) 83.1(1).

nuclear complex PPh_4-*mer*-$[Fe(bpca)_3(CN)_3]\cdot H_2O$ (**1**) [PPh_4^+ = tetraphenylphosphonium cation and $bpca^-$ = bis(pyridylcarbonyl)amidate anion] which reacts with $[Mn(H_2O)_6]^{2+}$ to yield the ladder-like chain compound $\{[Fe^{III}(bpca)(\mu\text{-}CN)_3]Mn^{II}(H_2O)_3\}[Fe^{III}(bpca)(CN)_3]\cdot 3H_2O$ (**2**). Both compounds were characterized by IR spectroscopy, variable-temperature magnetic measurements, and X-ray structural analysis.[14]

The crystal structure of **1** consists of *mer*-$[Fe(bpca)(CN)_3]^-$ anions (see Figure 1), uncoordinated tetraphenylphosphonium cations, and crystallization water molecules. The iron atom has a slightly distorted octahedral coordination geometry, its symmetry being close to C_{2v}. The Fe−N(bpca) bond distances vary in the range 1.893(2)−1.959(2) Å, values which are considerably shorter than those found in the high-spin iron(III) mononuclear complexes $[Fe(bpca)Cl_2(H_2O)]\cdot Me_2CO$ [2.076(4)−2.124(4) Å][18a] and $[Fe(bpca)Cl_2(ROH)]$ (R = Me, Et) [2.0767(15)−2.1269(16) Å].[18b] Good agreement is observed between the Fe(1)−C(cyano) bond distances of **1** [1.937(3)−1.951(3) Å] and those reported for the low-spin iron(III) complex PPh_4-*fac*-$[Fe\{HB(pz)_3\}(CN)_3]\cdot H_2O$ [$HB(pz)_3^-$ = hydrotris(1-pyrazolyl)borate] [1.910(6)−1.929(7) Å].[7] These features together with the presence of the tetraphenylphosphonium cation in the structure of **1**, the value of the magnetic moment at room temperature (μ_{eff} ca. 2.4 μ_B), and the cyanide stretching frequency [ca. 2126s cm^{-1} in **1** versus 2123s cm^{-1} in PPh_4-*fac*-$[Fe\{HB(pz)_3\}(CN)_3]\cdot H_2O$] demonstrate the low-spin character of the iron(III) in **1**. The PPh_4^+ cations are grouped by pairs exhibiting the offset face to face interaction pattern with a P···P separation of 7.039 Å (see Figure S1 in the Supporting Information).[19] The crystallization water molecule [O(3)] forms hydrogen bonds with a carbonyl-bpca atom [O(1)] of one $[Fe(bpca)(CN)_3]^-$ unit and a cyanide-nitrogen [N(1a); (a) = 1 − *x*, 2 − *y*, −*z*] of a symmetry related unit [2.943(3) and 2.876(4) Å for O(3)···O(1) and O(3)···N(1a)] leading to pairs of anions. The intradimer iron−iron separation is 8.503(1) Å, a value which is somewhat longer than the shortest interdimer Fe···Fe distance [8.245(1) Å for Fe(1)···Fe(b); (b) = −*x*, 2 − *y*, −*z*].

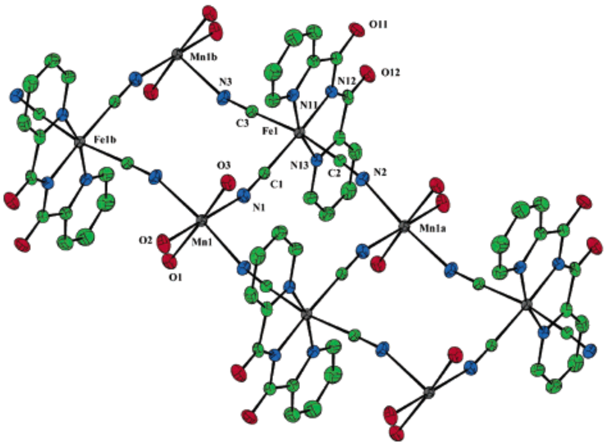

Figure 2. A view of the ladder-like chain of **2**. Selected bond lengths [Å] and angles [deg]: Fe(1)−C(1) 1.947(2)−1.952(2), Fe(1)−N 1.896(2)−1.970(2), Mn(1)−O 2.186(2)−2.218(2), Mn(1)−N 2.201(2)−2.222(2), N(11)−Fe(1)−N(12) 82.78(9), N(11)−Fe(1)−N(13) 165.05(9), N(12)−Fe(1)−N(13) 82.52(8), N(12)−Fe(1)−C(1) 177.22(9), C(2)−Fe(1)−C(3) 168.3(1), O(1)−Mn(1)−O(3) 170.22(7), O(2)−Mn(1)−N(1) 175.70(8), N(2a)−Mn(1)−N(2b) 173.93(9) [symmetry code: (a) = 1 − *x*, 1 − *y*, 1 − *z*; (b) = −*x*, 1 − *y*, 1 − *z*].

The structure of complex **2** is made up of cationic $[Fe^{III}(bpca)(\mu\text{-}CN)_3Mn^{II}(H_2O)_3]^+$ bimetallic ladder-like chains (see Figure 2), anionic $[Fe^{III}(bpca)(CN)_3]^-$ units (Figure S2), and crystallization water molecules. The chains run parallel to the *x* axis, and alternating stacking of chains and anions occurs along the *z* axis. The chains grow in the *xy* plane through an extensive network of hydrogen bonds involving the carbonyl-bpca atoms [O(11) and O(12)] and two coordinated [O(1) and O(2)] and two crystallization [O(100) and O(111)] water molecules (Figure S3). Additional hydrogen

---

(13) Smith, J. A.; Galán-Mascarós, J. R.; Clérac, R.; Dunbar, K. *Chem. Commun.* **2000**, 1077.

(14) Crystallographic analyses for **1** ($C_{39}H_{30}FeN_6O_3P$): $T = 295$ K, triclinic, space group $P\bar{1}$, $a = 8.787(2)$ Å, $b = 15.100(3)$ Å, $c = 15.158(3)$ Å, $\alpha = 60.24(1)°$, $\beta = 83.07(2)°$, $\gamma = 80.52(2)°$, $U = 1720.4(7)$ Å^3, $Z = 2$, $\rho_{calcd} = 1.39$ g cm^{-3}, $\mu = 5.28$ cm^{-1}, $R1 = 0.0381$, $wR2 = 0.0456$ for 4158 observed reflections with $I > 3\sigma(I)$ (from the 7214 collected in the θ range 1−26°, 6740 were unique), 452 parameters, residual maximum and minimum in the final Fourier difference maps were 0.38 and −0.33 e Å^{-3}. For **2** ($C_{30}H_{27}Fe_2MnN_{12}O_{9.5}$): $T = 295$ K, triclinic, space group $P\bar{1}$, $a = 10.417(3)$ Å, $b = 12.614(3)$ Å, $c = 14.898(5)$ Å, $\alpha = 110.33(2)°$, $\beta = 96.46(3)°$, $\gamma = 94.54(2)°$, $U = 1809(1)$ Å^3, $Z = 2$, $\rho_{calcd} = 1.61$ g cm^{-3}, $\mu = 11.9$ cm^{-1}, $R1 = 0.0404$, $wR2 = 0.0466$ for 5791 observed reflections with $I > 3\sigma(I)$ (from the 7515 collected in the θ range 1−26°, 7100 were unique), 504 parameters, residual maximum and minimum in the final Fourier difference maps were 0.74 and −0.50 e Å^{-3}. Diffraction data of **1** and **2** were collected on an Enraf-Nonius CAD-4 diffractometer using graphite-monochromated Mo Kα radiation ($\lambda = 0.71069$ Å) and were corrected for Lorentz and polarization effects. An emprirical absorption correction was performed by the use of DIFABS[15] (**1**) and the Ψ-scan curve (**2**). The structures of **1** and **2** were solved by direct methods through SHELX-86[16] and subsequently refined by Fourier recycling. The final full-matrix least-squares refinement on *F* was done by the PC version of CRYSTALS.[17] All non-hydrogen atoms of **1** and **2** were refined anisotropically. All hydrogen atoms (except those of the water molecules which were found on a difference map in **1** and not introduced in **2**) were introduced in calculated positions and were allocated one overall isotropic thermal parameter.

(15) Walker, N.; Stuart, D. *Acta Crystallogr.* **1983**, *A39*, 156.

(16) Sheldrick, G. M. *SHELX-86: Program for Crystal Structure Solution*; University of Göttingen: Göttingen, Germany, 1996.

(17) Watkin, D. J.; Prout, C. K.; Carruthers, J. R.; Betteridge, P. W. *CRYSTALS*; Chemical Crystallography Laboratory, University of Oxford: Oxford, U.K., 1996; Issue 10.

(18) (a) Wocadlo, S.; Massa, W.; Folgado, J. V. *Inorg. Chim. Acta* **1993**, *207*, 199. (b) Kajiwara, T.; Ito, T. *Acta Crystallogr.* **2000**, *C56*, 22.

(19) Dance, I.; Scudder, M. *Chem. Eur. J.*, **1996**, *2*, 481.

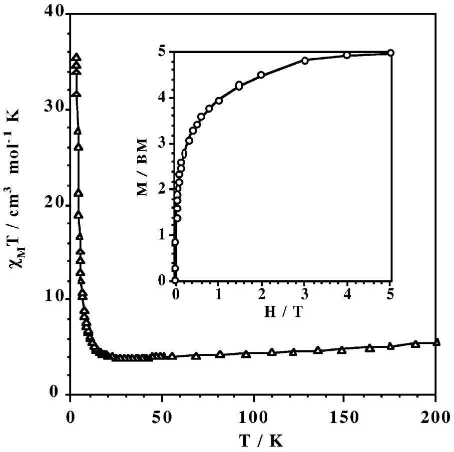

Figure 3. Temperature dependence of the $\chi_M T$ product for **2** [$H = 0.1$ T ($T > 50$ K) and 50 Oe ($T < 50$ K)]. The inset shows the M versus H plot of **2** at $T = 1.9$ K [(△, ○) experimental data; (—) eye guide lines].

bonds involving the uncoordinated [Fe^{III}(bpca)(CN)$_3$]$^-$ anions [through its three cyanide-nitrogens and the carbonyl-bpca oxygen O(14)] and two lattice [O(100) and O(103)] and the three coordinated [O(1) O(2) and O(3)] water molecules (Figure S4) lead to a three-dimensional structure. The anion of **1** is present in **2**, but here, it acts as a trismonodentate ligand [Fe(1)] through its three cyanide groups toward three manganese atoms and also as a counterion [Fe(2)]. Both iron atoms exhibit the same FeN$_3$C$_3$ distorted octahedral environment. The main distortion at the iron atom arises from the geometric constraints caused by the two five-membered chelate rings which are subtended by the tridentate bpca ligand [165.06(9)° and 165.86(9)° for N(11)−Fe(1)−N(13) and N(14)−Fe(2)−N(16), respectively; 165.7(1)° for N(4)−Fe(1)−N(6) in **1**]. The Fe−C(cyanide) bond lengths vary in a very narrow range [1.947(2)−1.952(2) (at Fe(1)) and 1.940(3)−1.957(3) Å (at Fe(2))], and the Fe−N(bpca) bond distances are very close at both iron atoms. The manganese atom [Mn(1)] has a MnN$_3$O$_3$ distorted octahedral environment with the three cyanide-nitrogen atoms in *mer*-position. The values of the Mn(1)−O(w) [2.186(2)−2.218(2) Å] and Mn(1)−N(cyanide) [2.201(2)−2.222(2) Å] bond lengths are as previously observed for this cation in related chains.[9,12] The Fe−C−N angles are quasilinear [176.2(2)−176.4(2)° (Fe(1)) and 176.4(3)−177.8(2)° (Fe(2))] whereas the Mn(1)−C−N ones are significantly bent [157.8(2)−162.3(2)°]. The intrachain metal−metal distances through the single cyano bridges are 5.179(1) Å [Fe(1)···Mn(1)], 5.241(1) Å [Fe(1)−Mn(1a); (a) = 1 − *x*, 1 − *y*, 1 − *z*], and 5.216(1) Å [Fe(1)···Mn(1b); (b) = −*x*, 1 − *y*, 1 − *z*].

The temperature dependence of $\chi_M T$ [χ_M is the magnetic susceptibility per Fe$_2$Mn unit] in the temperature range 200−1.9 K is shown in Figure 3. At 290 K, $\chi_M T$ is 5.70 cm^3 mol^{-1} K, a value which is as expected for a high-spin Mn(II) ($S = {}^5/_2$) and two low-spin Fe(III) ($S = {}^1/_2$) ions magnetically isolated. As the temperature is lowered, the $\chi_M T$ product smoothly decreases, exhibits a minimum at 30 K ($\chi_M T$ being 4.0 cm^3 mol^{-1} K), and further increases sharply to reach a maximum at 2.20 K ($\chi_M T_{max}$ being 35 cm^3 mol^{-1} K). The magnetization curve of **2** at 2.0 K (see inset of Figure 3) tends to a value of 5.0 μ_B at the maximum available magnetic field. Alternating current measurements of **2** reveal the presence of a maximum in the in-phase signal at 2.20 K (Figure S5) indicating the onset of magnetic ordering at such a low temperature. The shape of the $\chi_M T$ curve of **2** is typical of ferrimagnetic behavior: the decrease of $\chi_M T$ in the high-temperature range is due to both spin−orbit coupling of the two low-spin iron(III) ions and a significant intrachain antiferromagnetic interaction between low-spin Fe(III) and high-spin Mn(II) ions. This antiferromagnetic interaction is unambiguous because the value of $\chi_M T$ in the minimum (4.0 cm^3 mol^{-1} K) is well below that expected for two low-spin Fe(III) and one high-spin Mn(II) ions magnetically noninteracting, and in addition, the saturation value of the magnetization (5.0 μ_B) is as expected for a spin $S = 2$ arising from an antiferromagnetically coupled Mn(II)−Fe(III) pair ($S_{Mn} - S_{Fe} = {}^5/_2 - {}^1/_2 = 2$) plus an isolated low-spin Fe(III) ($S_{Fe} = {}^1/_2$).

DFT type calculations[20] on the [Fe(bpca)(CN)$_3$]$^-$ precursor show that its magnetic orbital is defined by a d_{xy} orbital lying in the plane of the three cyanide groups [the *x* and *y* axes being roughly defined by the N(5)−Fe(1)−C(3) and C(1)−Fe(1)−C(2) vectors; see Figure S6] with a large density value on the metal ion (1.033) and a small delocalization on a p atomic orbital centered on the nitrogen atom of the cyanide groups (0.036). So, although both ferro- and antiferromagnetic contributions are involved in the magnetic coupling between a high-spin Mn(II) ($t_{2g}{}^3e_g{}^2$) and a low-spin Fe(III) ($t_{2g}{}^5e_g{}^0$), it seems that the antiferromagnetic t_{2g}−t_{2g} ones are dominant in **2**. The lack of a theoretical model to analyze the magnetic properties of the bimetallic ladder-like chain present in **2** precludes any estimation of the antiferromagnetic coupling involved. In the near future, the use of the *mer*-[Fe(bpca)(CN)$_3$]$^-$ unit as a ligand toward coordinatively unsaturated metal complexes would provide a wide family of stereochemically controlled cyanide-bridged heterometallic magnetic assemblies.

Acknowledgment. This work was supported by the TMR Program from the European Union (Contract ERBFM-RXCT98-0181) and the Ministerio Español de Ciencia y Tecnología (Project BQU-2001-2928).

Supporting Information Available: Additional Figures S1−S6 and synthetic details (PDF) and crystallographic data in CIF format. This material is available free of charge via the Internet at http://pubs.acs.org.

IC030284Z

---

(20) Frisch, M. J.; Trucks, G. W.; Schlegel, H. B.; Scuseria, G. E.; Robb, M. A.; Cheeseman, J. R.; Zakrzewski, V. G.; Montgomery, J. A., Jr.; Stratmann, R. E.; Burant, J. C.; Dapprich, S.; Millam, J. M.; Daniels, A. D.; Kudin, K. N.; Strain, M. C.; Farkas, O.; Tomasi, J.; Barone, V.; Cossi, M.; Cammi, R.; Mennucci, B.; Pomelli, C.; Adamo, C.; Clifford, S.; Ochterski, J.; Petersson, G. A.; Ayala, P. Y.; Cui, Q.; Morokuma, K.; Malick, D. K.; Rabuck, A. D.; Raghavachari, K.; Foresman, J. B.; Cioslowski, J.; Ortiz, J. V.; Stefanov, B. B.; Liu, G.; Liashenko, A.; Piskorz, P.; Komaromi, I.; Gomperts, R.; Martin, R. L.; Fox, D. J.; Keith, T.; Al-Laham, M. A.; Peng, C. Y.; Nanayakkara, A.; Gonzalez, C.; Challacombe, M.; Gill, P. M. W.; Johnson, B. G.; Chen, W.; Wong, M. W.; Andres, J. L.; Head-Gordon, M.; Replogle, E. S.; Pople, J. A. *Gaussian 98*, revision A.11; Gaussian, Inc.: Pittsburgh, PA, 1998.